Ann Univ Ferrara (2007) 53:199–215
DOI 10.1007/s11565-007-0013-1

Efficient implementation of WENO schemes to nonuniform meshes

Nelida Črnjarić-Žic · Senka Maćešić · Bojan Crnković

Received: 29 October 2005 / Accepted: 20 November 2006 / Published online: 3 October 2007

Abstract Most of the standard papers about the WENO schemes consider their implementation to uniform meshes only. In that case the WENO reconstruction is performed efficiently by using the algebraic expressions for evaluating the reconstruction values and the smoothness indicators from cell averages. The coefficients appearing in these expressions are constant, dependent just on the scheme order, not on the mesh size or the reconstruction function values, and can be found, for example, in Jiang and Shu (J Comp Phys 126:202–228, 1996). In problems where the geometrical properties must be taken into account or the solution has localized fine scale structure that must be resolved, it is computationally efficient to do local grid refinement. Therefore, it is also desirable to have numerical schemes, which can be applied to nonuniform meshes. Finite volume WENO schemes extend naturally to nonuniform meshes although the reconstruction becomes quite complicated, depending on the complexity of the grid structure. In this paper we propose an efficient implementation of finite volume WENO schemes to nonuniform meshes. In order to save the computational cost in the nonuniform case, we suggest the way for precomputing the coefficients and linear weights for different orders of WENO schemes. Furthermore, for the smoothness indicators that are defined in an integral form we present the corresponding algebraic expressions in which the coefficients obtained as a linear combination of divided differences arise. In order to validate the new implementation, resulting schemes are applied in different test examples.

N. Črnjarić-Žic (✉) · S. Maćešić · B. Crnković
Faculty of Engineering, University of Rijeka, Rijeka, Croatia
e-mail: nelida@riteh.hr

S. Maćešić
e-mail: senka.vukovic@ri.t-com.hr

B. Crnković
e-mail: bojan.crnkovic@riteh.hr

Keywords Nonuniform mesh · Finite volume WENO schemes · Hyperbolic balance law · Open-channel flow equations · Allievi's equations

Mathematics Subject Classification (2000) 35L65 · 65M99 · 76M12

1 Introduction

In solving engineering problems modelled by hyperbolic balance laws, we often encounter situations in which the complicated geometry or the solution structure must be taken into account. In those cases it would be desirable to apply high order accurate numerical schemes, which could be used on nonuniform meshes. The numerical schemes satisfying stated requirements are finite volume WENO schemes. The generalization of their original version developed for hyperbolic conservation laws to the balance laws with geometrical source term is given in [3]. With the proposed extension the well-balanced numerical schemes, which preserve exactly some steady state solutions are obtained, and the balancing property is maintained even in the nonuniform mesh case. We made a similar extension of the finite difference WENO schemes in [8,9], but unfortunately, their high order accuracy is not maintained when applied to the nonuniform meshes [5].

In this paper we are interested in implementing efficiently the finite volume WENO schemes to the nonuniform meshes. However, in most of the papers about the WENO schemes, only their implementation to the uniform meshes is described [5,7]. In that case the WENO reconstruction is performed efficiently by using the algebraic expressions for evaluating the reconstruction values and the smoothness indicators from cell averages. The coefficients appearing in these expressions are constant, dependent just on the scheme order and not on the mesh size or the reconstruction function values [5]. This is not the case when the nonuniform mesh is used. From a brief description of the WENO reconstruction algorithm, given in Sect. 1.1, which is the base of WENO schemes, it is clear that the reconstruction algorithm is quite complicated and dependent on the grid structure. If the described algorithm is applied, the scheme becomes computationally too expensive and inefficient, since the WENO reconstruction must be performed at each time step of the numerical scheme. As we already mentioned, in the uniform mesh case the computational cost of the algorithm can be reduced by using the corresponding expressions with constant coefficient not dependent on the mesh size or the reconstruction function values. In this paper, we try to obtain similar expressions and procedures in the nonuniform mesh case. In Sect. 1.2 we suggest the way for precomputing the coefficients and linear weights, which depend now on the mesh size, but do not depend on the function values, so their values remain same at each time step. In that way the computational time for this part of the algorithm stays equal to the one used on the uniform mesh. However, when the smoothness indicators are evaluated we fail to obtain a similar algorithm as in the uniform mesh case. While on the uniform mesh there exists an algebraic expression with constant coefficients for evaluating their values, in the nonuniform mesh case we express the smoothness indicators as a combination of divided differences of the considered function. This

technique increases the computational cost of the scheme when compared with the uniform mesh case, since at each time step the divided differences must be evaluated.

The complete algorithm of WENO reconstruction proposed in Sect. 1 is then used in finite volume WENO schemes that are described in Sect. 2. Finally, their implementation to nonuniform meshes on different problems is considered in Sect. 3.

2 WENO algorithm on nonuniform meshes

2.1 WENO reconstruction algorithm

Assume we have the partition of an interval $[a, b]$

$$a = x_{\frac{1}{2}} < x_{\frac{3}{2}} < \cdots < x_{N-\frac{1}{2}} < x_{N+\frac{1}{2}} = b. \tag{2.1}$$

With the given partition the cells $I_i = [x_{i-\frac{1}{2}}, x_{i+\frac{1}{2}}]$ are defined. We denote with Δx_i the size of the cell I_i, with $x_i = \frac{x_{i-\frac{1}{2}}+x_{i+\frac{1}{2}}}{2}$ its centre, and the maximum cell size with $\Delta x = \max_{1\le i\le N} \Delta x_i$.

We consider the following reconstruction problem. Suppose that the cell averages $\overline{v}_i$ of the function $v(x)$, $\overline{v}_i = \frac{1}{\Delta x_i}\int_{x_{i-\frac{1}{2}}}^{x_{i+\frac{1}{2}}} v(x)dx,\ i = 1, \ldots, N$, in all the cells I_i are known. We are interested in the high order approximation to the pointwise values $v(x)$ of the function v in the ith cell. More precisely, we want to find the polynomial $p_i(x)$ of degree at most $r-1$ for each cell $I_i,\ i = 1, \ldots, N$, which is rth order accurate approximation to the function v in the cell I_i

$$p_i(x) = v(x) + \mathcal{O}(\Delta x^r), \quad x \in I_i. \tag{2.2}$$

Additionally, we require that our reconstructing polynomial satisfies

$$\frac{1}{\Delta x_i}\int_{I_j} p_i(\xi)d\xi = \overline{v}_j, \quad j = i-r+1+s, \ldots, i+s;\ s = 0, \ldots, r-1. \tag{2.3}$$

In fact, we can reconstruct r polynomials $p_i^s(x),\ s = 0, \ldots, r-1$ satisfying requirements (2.2) and (2.3). They are obtained from the interpolation procedure over the stencils

$$S_{r,s}(i) = \{I_{i-r+s+1}, \ldots, I_{i+s}\}, \quad s = 0, \ldots, r-1. \tag{2.4}$$

Each stencil consists from r consecutive cells and contains the cell I_i.

The polynomials $p_i^s(x),\ s = 0, \ldots, r-1$ are determined as described in this paragraph. First, we look at the primitive function $V(x) = \int_a^x v(\xi)d\xi$. Notice that we know the values $V(x)$ at the cell boundaries exactly

$$V(x_{i+\frac{1}{2}}) = \sum_{j=1}^{i}\int_{j-\frac{1}{2}}^{j+\frac{1}{2}} v(\xi)d\xi = \sum_{j=1}^{i}\overline{v}_j\Delta x_j. \tag{2.5}$$

Thus, we can find the rth degree polynomial $P_i^s(x)$ that interpolates $V(x)$ at the boundary points $x_{i-r+s+\frac{1}{2}}, \ldots, x_{i+s+\frac{1}{2}}$ of the cells contained in the stencil $S_{r,s}(i)$. The polynomial $p_i^s(x) = P_i^{s\prime}(x)$ then satisfies the requirements (2.2) and (2.3). The proof can be found in [7]. The practical issue of determining the values $p_i^s(x)$ is given in the next subsection.

As we already said, an rth order approximation to the function v in the ith cell can be determined for each stencil $S_{r,s}(i),\ s = 0, \ldots, r-1$. However, the stencils $S_{r,s}(i),\ s = 0, \ldots, r-1$ compose one larger stencil $\mathcal{T}(i)$

$$\mathcal{T}(i) = \bigcup_{s=0}^{r-1} S_{r,s}(i) \tag{2.6}$$

with $2r-1$ cells. By following the previously described procedure we can find $(2r-2)$th degree polynomial $q_i(x)$ associated to the stencil $\mathcal{T}(i)$, which approximates the function $v(x)$ with the order $2r-1$ in all the points of the ith cell, and furthermore satisfies (2.3) for every $I_j \in \mathcal{T}(i)$. Moreover, for each point $x \in I_i$ there exist constants $C_{r,s}(x)$ such that

$$q_i(x) = \sum_{s=0}^{r-1} C_{r,s}(x)\, p_i^s(x). \tag{2.7}$$

Thus, for an arbitrary point $x \in I_i$, we can obtain $(2r-1)$th order accurate approximation to the function value $v(x)$ as the linear combination of its rth order approximations. Again, the practical evaluation of the values $C_{r,s}(x)$ will be described in the next subsection.

WENO (weighted essentially non-oscillatory) reconstruction is the improvement of the described polynomial reconstruction. This improvement is based on the idea of avoiding spurious oscillations, which can appear near discontinuities. In order to achieve that, some modifications of the algorithm must be introduced. Instead of taking the polynomial value $q_i(x)$ as the high order approximation to the value $v(x)$ at the point $x \in I_i$, we take

$$v_r(x) = \sum_{s=0}^{r-1} \omega_{r,s}(x)\, p_i^s(x). \tag{2.8}$$

The crucial step in obtaining non-oscillatory reconstruction is the choice of weights $\omega_{r,s}(x)$. For the function, which is smooth in the stencil $S_{r,s}(i)$, the appropriate condition would be

$$\omega_{r,s}(x) = C_{r,s}(x) + \mathcal{O}(\Delta x^{r-1}), \quad s = 0, \ldots, r-1. \tag{2.9}$$

It can be proved that if (2.9) is valid, $v_r(x)$ is the approximation of the order of accuracy $(2r-1)$ to the value $v(x)$ [7]. If the discontinuity appears inside the stencil $S_{r,s}(i)$, we require the weight $\omega_{r,s}(x)$ to be small (near zero), so the influence of the polynomial that possibly contains oscillations becomes small. In this way the oscillations are avoided and the non-oscillatory reconstruction is achieved. The weights $\omega_{r,s}(x)$ are

defined with

$$\omega_{r,s}(x) = \frac{\alpha_{r,s}(x)}{\sum_{j=0}^{r-1} \alpha_{r,j}(x)}, \quad \alpha_{r,s}(x) = \frac{C_{r,s}(x)}{(\epsilon + IS_{r,s})^2}, \quad s = 0, \ldots, r-1. \tag{2.10}$$

Parameter ϵ is introduced to avoid that the denominator becomes zero and is usually equal to 10^{-6}. Coefficients $\omega_{r,s}(x)$ depend on the *smoothness indicators* $IS_{r,s}$ which are some sort of the measure of the smoothness of the polynomial $p_i^s(x)$ over the stencil I_i. They are usually taken as

$$IS_{r,s} = \sum_{l=1}^{r-1} \int_{I_i} \Delta x^{2l-1} \left(\frac{d^l p_i^s(x)}{dx^l} \right)^2 dx. \tag{2.11}$$

In the uniform mesh case expressions for efficiently evaluating the smoothness indicators are the combination of the average function values with constant coefficients (see [5]). In the nonuniform mesh case, we propose to use the procedure described in the next subsection.

For additional informations about the WENO reconstruction we refer to [5,7].

2.2 Implementation of the WENO reconstruction

Now, we are interested in the practical implementation of the described WENO algorithm.

First, the values of the polynomials $p_i^s(x)$ must be determined. If the interpolating polynomial $P_i^s(x)$ of the function $V(x)$ at the cell boundaries is written in Lagrange form

$$P_i^s(x) = \sum_{m=0}^{r} V(x_{i-r+s+m+\frac{1}{2}}) \prod_{l=0,\, l\neq m}^{r} \frac{x - x_{i-r+s+l+\frac{1}{2}}}{x_{i-r+s+m+\frac{1}{2}} - x_{i-r+s+l+\frac{1}{2}}}, \tag{2.12}$$

for the polynomial $p_i^s(x) = P_i^{s\prime}(x)$, the expression

$$p_i^s(x) = \sum_{j=0}^{r-1} a_{r,s,j}(x) \overline{v}_{i-r+1+s+j} \tag{2.13}$$

where

$$a_{r,s,j}(x) = \sum_{m=j+1}^{r} \frac{\sum_{l=0,\, l\neq m}^{r} \prod_{q=0,\, q\neq l,m}^{r} (x - x_{i-r+s+q+\frac{1}{2}})}{\prod_{l=0,\, l\neq m}^{r} (x_{i-r+s+m+\frac{1}{2}} - x_{i-r+s+l+\frac{1}{2}})} \Delta x_{i-r+1+s+j} \tag{2.14}$$

can be obtained (see [7] for details). It follows from (2.13) that the polynomial value at an arbitrary point $x \in I_i$, $p_i^s(x)$, can be determined as the linear combination of the cell average values of the given function. The coefficients $a_{r,s,j}(x)$ depend on the grid

structure, considered stencil, and the point x, but do not depend on the reconstruction function values.

A similar expression for $q_i(x)$ on a bigger stencil $\mathcal{T}(i)$ as for the polynomials $p_i^s(x)$ is valid

$$q_i(x) = \sum_{k=0}^{2r-2} \widetilde{a}_{r,k}(x)\overline{v}_{i-r+1+k}, \tag{2.15}$$

where

$$\widetilde{a}_{r,k}(x) = \sum_{m=k+1}^{2r-2} \frac{\sum_{l=0,\, l\neq m}^{2r-2} \prod_{q=0,\, q\neq l,m}^{2r-2} (x - x_{i-r+s+q+\frac{1}{2}})}{\prod_{l=0,\, l\neq m}^{2r-2} (x_{i-r+s+m+\frac{1}{2}} - x_{i-r+s+l+\frac{1}{2}})} \Delta x_{i-r+1+k}. \tag{2.16}$$

Therefore, to obtain the expressions for evaluating the coefficient $C_{r,s}(x)$, which are connected with the polynomials $p_i^s(x)$, $s = 0, \ldots, r-1$ and $q_i(x)$ through the relation (2.7), we include (2.13) and (2.15) into (2.7)

$$\begin{aligned}
\sum_{k=0}^{2r-2} \widetilde{a}_{r,k}(x)\overline{v}_{i-r+1+k} &= \sum_{s=0}^{r-1} C_{r,s}(x) \sum_{j=0}^{r-1} a_{r,s,j}(x)\overline{v}_{i-r+1+s+j} \\
&= \sum_{j=0}^{r-1}\sum_{s=0}^{r-1} C_{r,s}(x) a_{r,s,j}(x)\overline{v}_{i-r+1+s+j} \\
&= \sum_{k=0}^{2r-2} \sum_{s=\max\{0,k-r+1\}}^{\min\{k,r-1\}} C_{r,s}(x) a_{r,s,k-s}(x)\overline{v}_{i-r+1+k}.
\end{aligned} \tag{2.17}$$

Then, by comparing left and right-hand side of the above equation, we can obtain a recursive algorithm for determining the values $C_{r,s}(x)$,

$$C_{r,s}(x) = \frac{\widetilde{a}_{r,s}(x) - \sum_{k=0}^{s-1} C_{r,k}(x) a_{r,k,s-k}(x)}{a_{r,s,0}(x)}, \quad s = 0, \ldots, r-1. \tag{2.18}$$

We refer to the coefficients $C_{r,s}(x)$ as to the optimal linear weights. Again, as the coefficients $a_{r,s,j}(x)$ and $\widetilde{a}_{r,k}(x)$, the coefficients $C_{r,s}(x)$ also depend just on the mesh geometry and not on the given function values. Therefore, all the coefficients $a_{r,s,j}(x)$, $\widetilde{a}_{r,k}(x)$, and $C_{r,s}(x)$ can be precomputed, so their evaluation does not affect the computational cost of the reconstruction. As we already mentioned in the introduction, in the uniform mesh case all the coefficients are constant, they depend just on the reconstruction order, chosen point x and not on the mesh size and the considered cell I_i.

In order to implement the main idea of the WENO reconstruction, the smoothness indicators, defined with (2.11) must be yet evaluated. Their values can be expressed as the combination of the average function values with coefficients that are in the nonuniform mesh case dependent on the grid structure. Since we do not know any efficient algorithm for precomputing them, the algorithm becomes to expensive. In

order to reduce the computational cost, we rather express the smoothness indicators as a combination of divided differences as will be described in following paragraph. In this paper, we present these expressions for the cases $r = 2, 3$ and 4.

First, we expand the polynomial $p_i^s(x)$ around the point $x_{i+\frac{1}{2}}$, i.e. for the rth order approximation we rewrite it in the form

$$p_i^s(x) = b_{s,0} + b_{s,1}(x - x_{i+\frac{1}{2}}) + b_{s,2}(x - x_{i+\frac{1}{2}})^2 + \cdots + b_{s,r-1}(x - x_{i+\frac{1}{2}})^{r-1}. \quad (2.19)$$

In the expressions for evaluating the coefficients $b_{s,k}$, $k = 0, \ldots, r-1$, the divided differences with the average function values appear. We introduce the notations

$$v[j][r] = \overline{v}[j, j+1, \ldots, j+r-1]$$

where the right-hand side is defined recursively with $\overline{v}[j] = \overline{v}_j$ and

$$\overline{v}[j, j+1, \ldots, j+r] = \frac{\overline{v}[j+1, \ldots, j+r] - \overline{v}[j, j+1, \ldots, j+r-1]}{x_{j+r+\frac{1}{2}} - x_{j-\frac{1}{2}}}. \quad (2.20)$$

For $r = 2, 3$, and 4, the terms $b_{s,r-k}$, $k = 1, \ldots, r-1$, belonging to the polynomials $p_i^s(x)$ are defined with

$$\begin{aligned}
b_{s,r-1} &= r\, v[m][r] \\
b_{s,r-2} &= (r-1)v[m][r-1] + (r-1)\sum_{j=0}^{r-1}(x_{i+\frac{1}{2}} - x_{m+j-\frac{1}{2}})v[m][r] \quad (2.21)\\
b_{s,r-3} &= (r-2)v[m][r-2] + (r-2)\sum_{j=0}^{r-2}\left((x_{i+\frac{1}{2}} - x_{i-r+1+s+j-\frac{1}{2}})\cdot\right. \\
&\quad \left.\cdot\left(v[m][r-1] + \sum_{q=0}^{r-2-j}(x_{i+\frac{1}{2}} - x_{i+s-q-\frac{1}{2}})v[m][r]\right)\right)
\end{aligned}$$

where $m = i - r + 1 + s$. Finally, the expressions for evaluating the smoothness indicators are given with

$$r = 2 : IS_{r,s} = b_{s,1}^2 \Delta x_i^2, \quad (2.22)$$

$$r = 3 : IS_{r,s} = \left(b_{s,1}^2 - 2b_{s,1}b_{s,2}\Delta x_i + \frac{16}{3}b_{s,2}^2\Delta x_i^2\right)\Delta x_i^2, \quad (2.23)$$

$$\begin{aligned}
r = 4 : IS_{r,s} = \left(b_{s,1}^2 - 2b_{s,1}b_{s,2}\Delta x_i + \left(\frac{16}{3}b_{s,2}^2 + 2b_{s,1}b_{s,3}\right)\Delta x_i^2\right. \quad (2.24)\\
\left. -15b_{s,2}b_{s,3}\Delta x_i^3 + \frac{249}{5}b_{s,3}^3\Delta x_i^4\right)\Delta x_i^2.
\end{aligned}$$

With this, the complete description of the reconstruction procedure on the nonuniform mesh is given. However, the computational cost of the proposed reconstruction increases in comparison with the reconstruction on the uniform mesh, since the divided differences and the coefficients defined with (21), needed for evaluating the smoothness indicators (2.22)–(2.25), must be determined at each time step.

The described procedure can be applied in approximating the considered function in an arbitrary point of the interval using the known average values. Notice that when we are interested in the approximation at the point $x_{i+\frac{1}{2}}$, which is the boundary point of the intervals I_i and I_{i+1}, two different approximations can be obtained: one belonging to the cell I_i and the other one belonging to I_{i+1}. If we assign the stencils $S_{r,s}(i)$ to the boundary $i+\frac{1}{2}$ instead to the cell I_i, for approximating the function on the considered boundary, the stencils $S_{r,s}(i),\ s=0,\ldots,r$ are used. For $s=0,\ldots,r-1$ we obtain the high order approximation from the left-hand side of the boundary

$$v^{-}_{i+\frac{1}{2},r}=\sum_{s=0}^{r-1}\omega_{r,s}(x_{i+\frac{1}{2}})\,p^{s}_{i}(x_{i+\frac{1}{2}}),$$

and for $s=1,\ldots,r$ we obtain the high order approximation from the right-hand side of the boundary

$$v^{+}_{i+\frac{1}{2},r}=\sum_{s=0}^{r-1}\omega_{r,s}(x_{i+\frac{1}{2}})\,p^{s}_{i+1}(x_{i+\frac{1}{2}})=\sum_{s=1}^{r}\omega_{r,s}(x_{i+\frac{1}{2}})\,p^{s}_{i}(x_{i+\frac{1}{2}}).$$

The expressions for evaluating both values can be written together as

$$v^{\pm}_{i+\frac{1}{2},r}=\sum_{s=s^{\pm}_{min}}^{s^{\pm}_{max}}\sum_{j=0}^{r-1}\omega^{\pm}_{r,s}(x_{i+\frac{1}{2}})a_{r,s,j}(x_{i+\frac{1}{2}})\overline{v}_{i-r+1+s+j},\tag{2.25}$$

for $s^{-}_{min}=0$, $s^{-}_{max}=r-1$, $s^{+}_{min}=1$, and $s^{+}_{max}=r$. When evaluating the left-hand side approximation $v^{-}_{i+\frac{1}{2},r}$ the complete previously described procedure must be applied, while for the right-hand side approximation $v^{+}_{i+\frac{1}{2},r}$, the new terms $C^{+}_{r,s}(x_{i+\frac{1}{2}})$, $\omega^{+}_{r,s}(x_{i+\frac{1}{2}})$, and $IS^{+}_{r,s}$ must be determined. $C^{+}_{r,s}(x_{i+\frac{1}{2}})$ are obtained as coefficients that belong to the stencils containing the cell I_{i+1} and to the polynomial value $q_{i+1}(x_{i+\frac{1}{2}})$, $IS^{+}_{r,s}$ are the smoothness indicators of the polynomials over the cell I_{i+1} and finally $\omega^{+}_{r,s}(x_{i+\frac{1}{2}})$ are obtained by taking the terms $IS^{+}_{r,s}$ instead of $IS_{r,s}$ in (2.10). When $IS^{+}_{r,s}$ are evaluated, the expressions (2.22)–(2.24) in which all the signs $-$ are replaced with $+$, and Δx_i with Δx_{i+1}, can be used.

3 Finite volume WENO scheme

The reconstruction described in the previous section is the base for the finite volume WENO schemes when solving the hyperbolic conservation and balance laws. For the considered one-dimensional balance law of the form

$$\frac{\partial \mathbf{u}}{\partial t} = -\frac{\partial \mathbf{f}(\mathbf{u}, x)}{\partial x} + \mathbf{g}(\mathbf{u}, x), \tag{3.1}$$

we look for the solution $\mathbf{u}(x, t)$. The general structure of the corresponding conservative scheme for solving (3.1) is

$$\frac{d\overline{\mathbf{u}}_i(t)}{dt} = -\frac{1}{\Delta x_i}\left(\widetilde{\mathbf{f}}_{i+\frac{1}{2}} - \widetilde{\mathbf{f}}_{i-\frac{1}{2}}\right) + \frac{1}{\Delta x_i}\mathbf{G}_i. \tag{3.2}$$

Here $\overline{\mathbf{u}}_i(t)$ denotes the approximation to the average value of the solution over the cell I_i at time t, $\widetilde{\mathbf{f}}_{i+\frac{1}{2}}$ is the numerical approximation to the value $\mathbf{f}(\mathbf{u}(x_{i+\frac{1}{2}}, t), x_{i+\frac{1}{2}})$, while $\mathbf{G}_i$ approximates the term $\int_{I_i} \mathbf{g}(\mathbf{u}(x, t), x)dx$. The left-hand side of the above equation, i.e. the time part, is solved by using the TVD Runge–Kutta time integration. The approximations of the terms on the right side of (3.2) are based on WENO reconstruction and on the solution of the generalized Riemann problem. Since at each time step the average values $\overline{\mathbf{u}}_i(t)$ are known, Riemann problem can be defined on each $(i + \frac{1}{2})$th cell boundary. The values $\mathbf{u}^-_{i+\frac{1}{2}}$ and $\mathbf{u}^+_{i+\frac{1}{2}}$, which approximate the exact value of the solution at the considered cell boundary can be determined using the WENO reconstructions. Then the corresponding Riemman problem should be solved. Since the exact values of such solution are not always available or inexpensive, the approximate Riemann solvers are used, i.e.

$$\widetilde{\mathbf{f}}_{i+\frac{1}{2}} = \mathbf{F}\left(\mathbf{u}^-_{i+\frac{1}{2}}, \mathbf{u}^+_{i+\frac{1}{2}}\right), \tag{3.3}$$

where $\mathbf{F}$ is the numerical flux function consistent with the physical flux. In this work the Roe and Lax–Friedrichs fluxes are used (see [3]). Furthermore, for approximating the geometrical part of the source term integral $\mathbf{G}_i$, the decomposed approach is applied, such that the exact conservation property is achieved [1,3].

In summary, we perform the following algorithm for the finite volume WENO scheme:

1. Precompute the coefficients $a_{r,s,j}(x_{i+\frac{1}{2}})$ and $C^{\pm}_{r,s}(x_{i+\frac{1}{2}})$ for $i = 0, \ldots, N,\ j = 0, \ldots, r-1,\ s = 0, \ldots, r$.
   At each time step:
2. Based on the precomputed coefficients and known cell average values $\overline{\mathbf{u}}_i$ evaluate, depending on the scheme order, the smoothness indicators (2.22)–(2.25). Then evaluate the weights $\omega^{\pm}_{r,s}(x_{i+\frac{1}{2}})$ by using (2.10), $i = 0, \ldots, N,\ s = 0, \ldots, r$.
3. Determine the $(2r-1)$th order approximations $\mathbf{u}^-_{i+\frac{1}{2}}$ and $\mathbf{u}^+_{i+\frac{1}{2}}$ by using (2.25).

4. Compute the numerical flux $\widetilde{\mathbf{f}}_{i+\frac{1}{2}}$ from (3.3) and the approximation $\mathbf{G}_i$ to the integral of the source term.
5. Use the obtained values in (3.2) and determine the new values $\overline{\mathbf{u}}_i$ at the next time step by applying the Runge–Kutta time integration. Go to step 2.

4 Numerical tests

We consider the application of the WENO schemes to nonuniform meshes on different type of problems that are modelled by the open-channel flow equations and Allievi's equations. We compare the obtained results with the analytical solutions or with the numerical solutions obtained on the uniform mesh. Also, the computational costs of the schemes used on nonuniform and uniform meshes are compared. Moreover, we present the results obtained by simulating real flow situations from engineering practice.

4.1 Open-channel flow equations

The water flows through a rectangular open channel of varying breadth and bed slope is modelled by system (3.1) where

$$\mathbf{u} = \begin{pmatrix} A \\ Q \end{pmatrix}, \mathbf{f} = \begin{pmatrix} Q \\ \frac{Q^2}{A} + g\frac{A^2}{2B} \end{pmatrix}, \mathbf{g} = \begin{pmatrix} 0 \\ g\frac{A^2}{2B^2}\frac{dB}{dx} - gA\frac{dz}{dx} - gAS_f \end{pmatrix}. \tag{4.1}$$

Here $A = A(x,t)$ is the wetted cross section area, $Q = Q(x,t)$ is the discharge, $B = B(x)$ is the channel width, g is the gravitational constant, and $z = z(x)$ is the bed level. Moreover, the relations $A = Bh$ and $Q = Av$ are valid, where $h = h(x,t)$ denotes the water depth and $v = v(x,t)$ the water velocity. The friction term S_f is defined with $S_f = \frac{M^2 Q|Q|}{A^2 R^{4/3}}$. Here $M = M(x)$ is the Manning's friction factor and $R = R(x, A)$ is the cross section hydraulic radius.

4.1.1 Rarefaction over a rectangular bump

This is a test that consists of the two rarefaction waves, but with an addition of a nontrivial topography. This test problem is proposed in [4]. The bottom topography is defined with

$$z(x) = \begin{cases} 1, & \text{if } 8.33 < x < 12.5 \\ 0, & \text{if } x < 8.32 \text{ or } x > 12.51 \end{cases}. \tag{4.2}$$

The initial water level height is $10m$, while the initial discharge is

$$Q(x,0) = \begin{cases} -350, & \text{if } x < 16.6 \\ 350, & \text{if } x > 16.8 \end{cases} \tag{4.3}$$

(see Fig. 1). In the given riverbed and discharge functions the defined constant values are connected with linear functions over the intervals, which are not included in

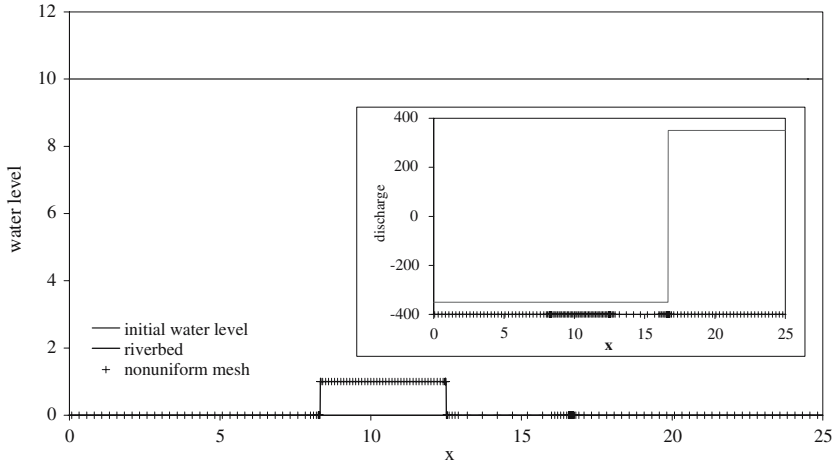

Fig. 1 Initial conditions and nonuniform mesh for the test 4.1.1

definitions (4.2) and (4.3). We use this test to illustrate the behaviour of our schemes in the quite complicated water flow situations. We compare the results obtained on the nonuniform mesh with 170 cells with the results obtained on the uniform mesh with 2500 cells. The cell size $\Delta x = 0.01m$ in the uniform mesh case is chosen such that all changes in the riverbed and in the initial data are taken into account. Hence, the initial data are on numerical level exactly defined. To satisfy the same conditions in the nonuniform mesh case, it is enough to refine the mesh just locally (see Fig. 1). We used the cell whose length varies from $0.01m$ to $0.5m$. The numerical results obtained with finite volume WENO scheme with $r = 2$ in different time moments are presented in Fig. 2. We can observe that the water level obtained on a quite coarse nonuniform grid agree very well with the results obtained on the much denser uniform mesh.

4.1.2 MacDonalds test example

MacDonald developed in [6] a very useful technique for constructing the steady-state test problems with the analytical solution. He considered the rectangular and trapezoidal channels with variable breadth and riverbed height. From the defined channel bottom width $B_0(x) = B(x, 0)$, side slope of the channel S, Manning friction factor $M = M(x)$, the proposed water depth $h(x)$, and constant discharge Q at the steady-state, one can obtain the bottom slope of the channel $z = z(x)$ corresponding to the imposed stationary solution. The equation, which connects mentioned values can be found in [6].

In this test example, taken from [6], the rectangular channel is considered. The width of the channel is defined with (Fig. 3)

$$B_0(x) = 10 - 5e^{-10\left(\frac{x}{200} - \frac{1}{2}\right)^2} \tag{4.4}$$

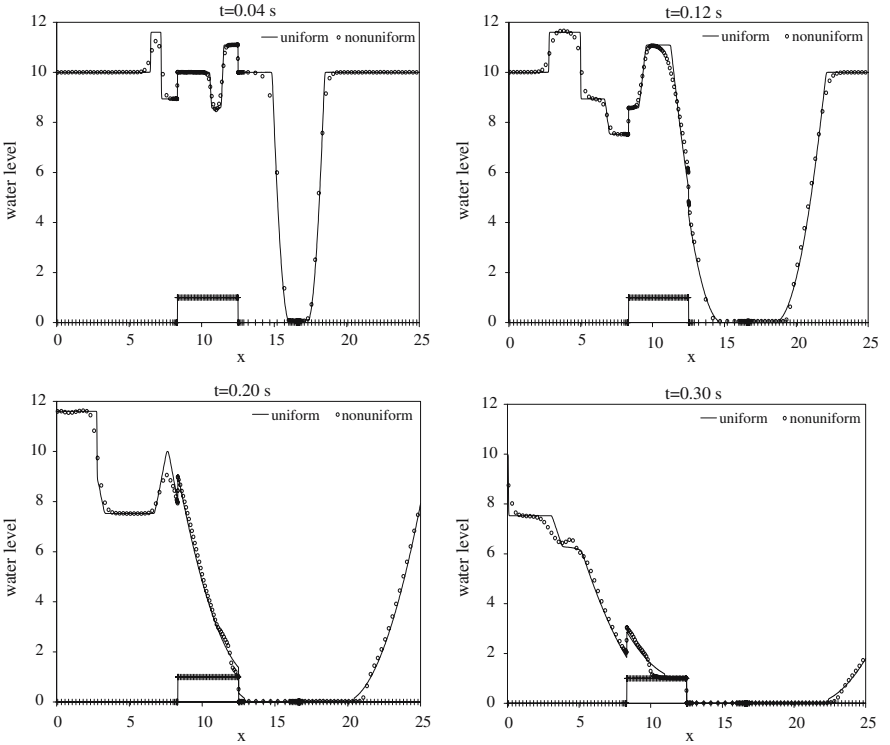

Fig. 2 Comparison of numerical results obtained with finite volume WENO scheme, $r = 2$ on uniform and nonuniform mesh. Water level at different time moments (test problem 4.1.1)

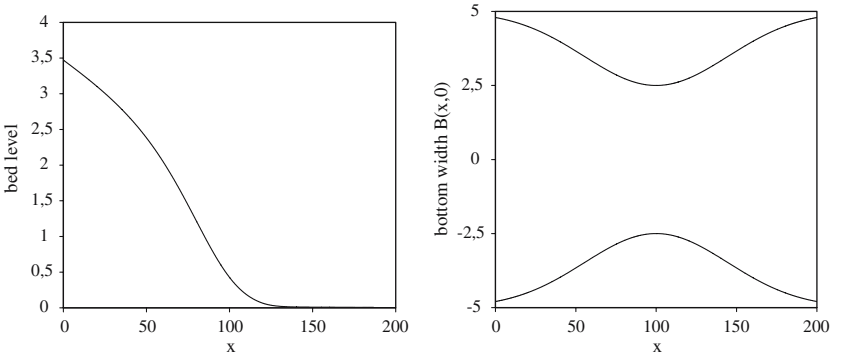

Fig. 3 Test problem 4.1.2. *Left* bed level, *right* width of the channel

and the water depth with

$$h(x) = \begin{cases} 0.7 + 0.3\left(e^{\frac{x}{200}} - 1\right), & x \le 120 \\ e^{-0.1(x-120)}\left(-0.154375 - 0.108189\frac{x-120}{80} - 2.014310\left(\frac{x-120}{80}\right)^2\right) \\ +1.5e^{-0.1\left(\frac{x}{200}-1\right)}, \qquad x > 120. \end{cases} \tag{4.5}$$

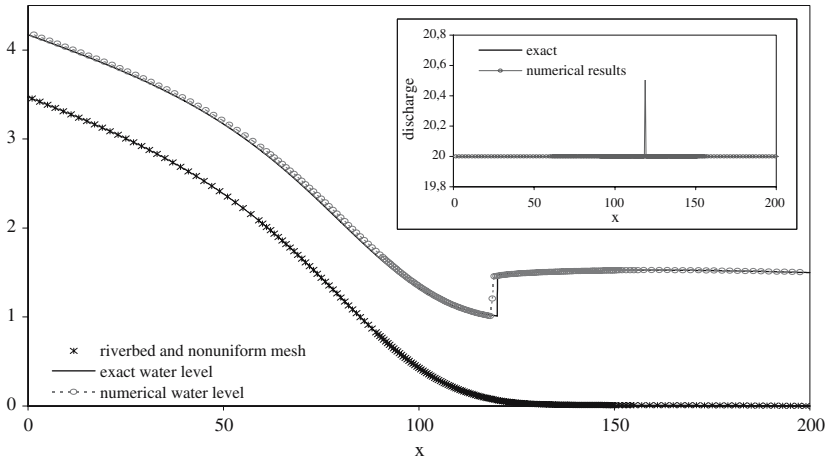

Fig. 4 Comparison of the numerical results obtained with the finite volume WENO scheme on nonuniform mesh with the analytical solution (test 4.1.2)

In order to obtain a stationary solution that corresponds to the constant discharge $Q = 20m^3/s$, constant Manning friction factor $M = 0.03$ and the water depth defined with (4.5), the height of the riverbed is determined as described in [6] and is presented in Fig. 3. The boundary conditions are defined with

$$Q(0,t) = 20m^3/s,\ h(0,t) = 0.7m,\ \text{ and }\ h(200,t) = 1.215485m. \tag{4.6}$$

In Fig. 4 the numerical results obtained with the finite volume WENO scheme on nonuniform mesh, $r = 3$, are compared to the exact solutions. In order to achieve a satisfactory approximation of the hydraulic jump occurring at $x = 120m$, the local mesh refinement is made. The cell sizes vary from $\Delta x = 0.05m$ to $\Delta x = 2m$ and increase toward the domain boundaries. The used mesh is presented in Fig. 4.

4.2 Allievi's equations

The Allievi's equations are used for modelling the pipe flow of a liquid with constant density ρ and are defined with

$$\mathbf{u} = \begin{pmatrix} p \\ Q \end{pmatrix}, \mathbf{f} = \begin{pmatrix} \frac{c^2\rho}{A} Q \\ \frac{A}{\rho} p \end{pmatrix}, \mathbf{g} = \begin{pmatrix} 0 \\ -g\rho \frac{dz}{dx} - \frac{\lambda Q|Q|}{2DA} \end{pmatrix}. \tag{4.7}$$

Here $p = p(x,t)$ denotes the pressure, $Q = Q(x,t)$ is the discharge, $z = z(x)$ the pipe level, $A = A(x)$ the cross section area, and $D = D(x)$ the pipe cross section diameter. The wave velocity c, which is in general determined by the elastic properties of the system, of the liquid, and of the system geometry, is constant. Moreover, the source term consists of two parts: the first one models the gravitational forces, while

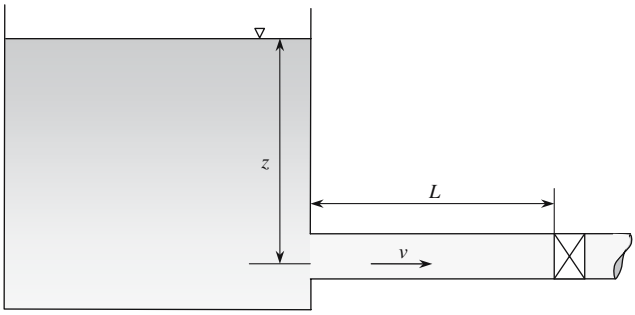

Fig. 5 A system for the ideal water hammer test 4.2.1

the second one belongs to the friction forces. For details about the model we refer to [2].

4.2.1 Ideal water hammer

The considered system consists from a horizontal, constant-diameter pipe leading from a reservoir to some unknown destination far downstream. A valve is placed a distance $L = 500m$ from the reservoir (see Fig.5). Friction in the pipe is assumed negligible. Water hammer will be introduced into the system by suddenly closing the valve.

For modelling the described situation, Allievi's equations are used. Furthermore, the initial and boundary conditions must be defined. Initially, it is assumed that $p(x, 0) = 3000kPa$ and $Q(x, 0) = 1m^3/s$. The reservoir is modelled by imposing the constant pressure at the upstream pipe boundary, while the valve closure is modelled by setting the discharge on the downstream pipe boundary to zero at $t = 0s$. In the defined system the shock wave that appears by closing the valve travels upstream with the velocity c, reaches the reservoir and then returns back. Since no energy losses are supposed in the system, the introduced disturbance periodically repeats.

In the considered test we compare the computational times of WENO schemes for uniform and nonuniform meshes. We actually take the same uniform mesh in both cases, but when the numerical schemes for nonuniform meshes were used, all the computations were performed as for the nonuniform mesh case. The computational times needed for obtaining the solution at $t = 2s$ are presented in Table 1.

4.2.2 The hydroelectric powerplant Rijeka

The task of the project was to calibrate the parameters of the mathematical model of the hydroelectric powerplant Rijeka according to the measured data. The longitudinal section of the hydroelectric powerplant Rijeka is presented in Fig. 6. The corresponding model consists of a reservoir, several pipes entering and leaving junctions, surge tank and turbine. The reservoir was modelled as an inflow boundary condition of a known pressure, i.e. $p(0, t)$ was defined, while the turbine was modelled as an outflow boundary condition of the known discharge, i.e. the function $Q(L, t)$ was defined. Both

Table 1 Computational times of finite volume WENO schemes for uniform/nonuniform meshes in test 4.2.1

Num. of cells	r	Uniform	Nonuniform	Increase of comp. time (%)
100	1	5.235	6.516	24.47
	2	5.688	6.047	6.31
	3	5.766	7.359	27.63
200	1	9.656	11.140	15.37
	2	10.156	12.219	20.31
	3	11.297	17.063	51.04
500	1	28.907	39.781	37.61
	2	33.531	46.640	39.09
	3	40.328	81.875	103.02

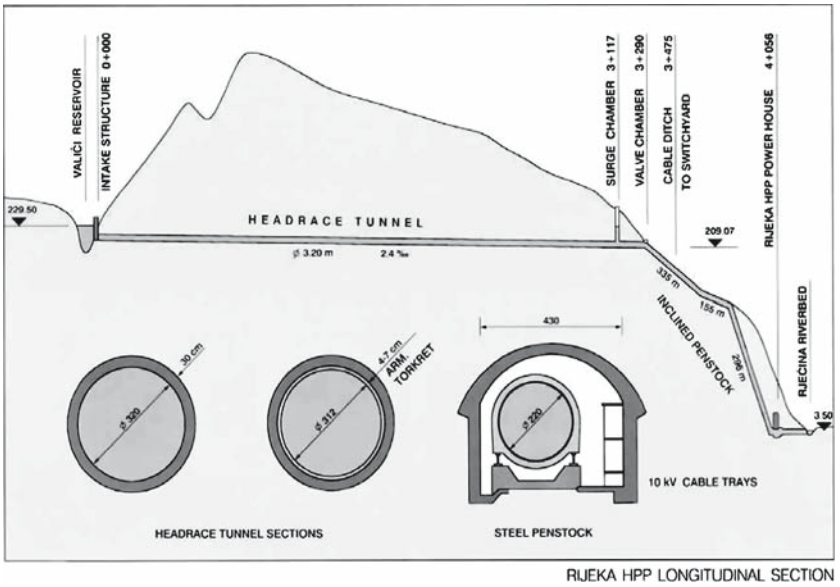

Fig. 6 The longitudinal section of Rijeka hydroelectric powerplant

boundary conditions we obtain from measurements. In order to calibrate the model, the elevation of the water at the surge tank was measured. The calibrated parameters were roughness coefficient, friction factor in pipes and friction factor in surge tank. In computations we use the nonuniform mesh, which is defined such that the exact geometry of pipes is taken into account (see Fig. 7). To achieve the same effect with the uniform mesh, a much denser mesh should be used.

The results presented in Fig. 8 show good agreement of the numerical results with the measured data.

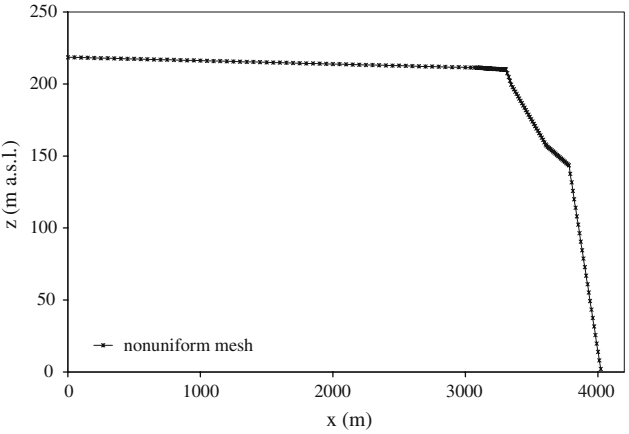

Fig. 7 The geometry of the pipes and the nonuniform mesh in test 4.2.2

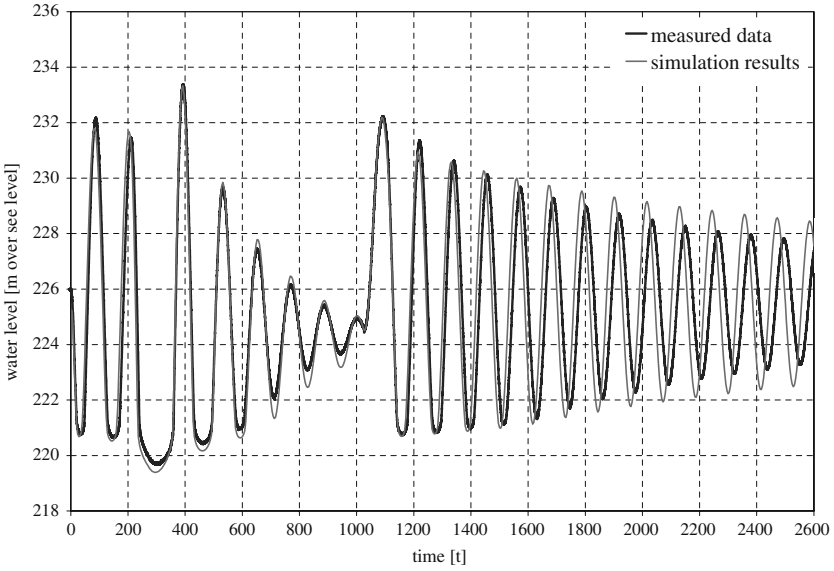

Fig. 8 Comparison of the simulated results with the measured data. Water level in surge tank obtained with the finite volume WENO scheme (test 4.2.2)

5 Concluding remarks

In real engineering problems that are modelled with hyperbolic balance laws there arise situations in which the nonuniform meshes must be used. In this work we consider the application of finite volume WENO schemes when solving such problems. Actually, we propose an efficient algorithm for the WENO reconstruction procedure, which is the base of the considered numerical schemes. With the given numerical problems we illustrate the use and the efficiency of the proposed numerical schemes.

References

1. Bermùdez, A., Vázquez, M.E.: Upwind methods for hyperbolic conservation laws with source terms. Comput. Fluids **23**(8), 1049 (1994)
2. Chaudhry, M.H.: Applied Hydraulic Transients. Van Nostrand Reinhold, New York (1987)
3. Črnjarić–Žic, N., Vuković, S., Sopta, L.: Balanced finite volume and central WENO schemes for the shallow water and the open-channel flow equations. J. Comput. Phys. **200**, 512 (2004)
4. Gallouët, T., Hérard, J.M., Seguin, N.: Some approximate Godunov schemes to compute shallow water equations with topography. Comput. Fluids **32**, 479–513 (2003)
5. Jiang, G.S., Shu, C.W.: Efficient implementation of weighted ENO schemes. J. Comput. Phys. **126**, 202–228 (1996)
6. MacDonald, I.: Analysis and computation of steady open channel flow. PhD Thesis, University of Reading. Available online on: http://www.extra.rdg.ac.uk/Maths/research/publications/Phd_theses/I_macdonald.asp (1996)
7. Shu, C.W.: Essentially non-oscillatory and weighted essentially non-oscillatory schemes for hyperbolic conservation laws. In: Cockburn, B., Johnson, C., Shu, C.W., Tadmor, E. (eds.) Advanced Numerical Approximation of Nonlinear Hyperbolic Equations. Lect. Notes in Math., vol. 160. Springer, Berlin, p. 325 (1998)
8. Vuković, S., Sopta, L.: ENO and WENO schemes with the exact conservation property for one-dimensional shallow water equations. J. Comput. Phys. **179**, 593 (2002)
9. Vuković, S., Črnjarić–Žic, N., Sopta, L.: WENO schemes for balance laws with spatially varying flux. J. Comput. Phys. **199**, 87 (2004)